AMERICAN SOCIETY FOR MICROBIOLOGY | Journal of Bacteriology®

RESEARCH ARTICLE

Roles of Alanine Dehydrogenase and Induction of Its Gene in *Mycobacterium smegmatis* under Respiration-Inhibitory Conditions

Ji-A Jeong,[a] Sae Woong Park,[b] Dahae Yoon,[c] Suhkmann Kim,[c] Ho-Young Kang,[a] Jeong-Il Oh[a]

[a]Department of Integrated Biological Science, Pusan National University, Busan, South Korea
[b]Department of Microbiology and Immunology, Weill Cornell Medical College, New York, New York, USA
[c]Department of Chemistry, Center for Proteome Biophysics and Chemistry Institute for Functional Materials, Pusan National University, Busan, South Korea

ABSTRACT Here we demonstrated that the inhibition of electron flux through the respiratory electron transport chain (ETC) by either the disruption of the gene for the major terminal oxidase (aa_3 cytochrome *c* oxidase) or treatment with KCN resulted in the induction of *ald* encoding alanine dehydrogenase in *Mycobacterium smegmatis*. A decrease in functionality of the ETC shifts the redox state of the NADH/NAD$^+$ pool toward a more reduced state, which in turn leads to an increase in cellular levels of alanine by Ald catalyzing the conversion of pyruvate to alanine with the concomitant oxidation of NADH to NAD$^+$. The induction of *ald* expression under respiration-inhibitory conditions in *M. smegmatis* is mediated by the alanine-responsive AldR transcriptional regulator. The growth defect of *M. smegmatis* by respiration inhibition was exacerbated by inactivation of the *ald* gene, suggesting that Ald is beneficial to *M. smegmatis* in its adaptation and survival under respiration-inhibitory conditions by maintaining NADH/NAD$^+$ homeostasis. The low susceptibility of *M. smegmatis* to bcc_1 complex inhibitors appears to be, at least in part, attributable to the high expression level of the *bd* quinol oxidase in *M. smegmatis* when the bcc_1-aa_3 branch of the ETC is inactivated.

IMPORTANCE We demonstrated that the functionality of the respiratory electron transport chain is inversely related to the expression level of the *ald* gene encoding alanine dehydrogenase in *Mycobacterium smegmatis*. Furthermore, the importance of Ald in NADH/NAD$^+$ homeostasis during the adaptation of *M. smegmatis* to severe respiration-inhibitory conditions was demonstrated in this study. On the basis of these results, we propose that combinatory regimens including both an Ald-specific inhibitor and respiration-inhibitory antitubercular drugs such as Q203 and bedaquiline are likely to enable a more efficient therapy for tuberculosis.

KEYWORDS alanine dehydrogenase, AldR transcriptional regulator, electron transport chain, gene expression, *Mycobacterium*, redox homeostasis, respiration

NAD(H)-dependent alanine dehydrogenase (EC 1.1.4.1; Ald) catalyzes the reductive amination of pyruvate to L-alanine and its reverse reaction. The oxidative deamination reaction catalyzed by Ald is required for mycobacteria to utilize alanine as a nitrogen source (1–3). In addition, Ald in mycobacteria has been suggested to be necessary for hypoxic growth by maintaining the redox balance of the NADH/NAD$^+$ pool via its reductive amination reaction (3–6). Ald proteins from *Mycobacterium tuberculosis* and *Mycobacterium smegmatis* are also known to catalyze the reductive amination of glyoxylate to glycine but not the reverse reaction (2, 7). The mycobacterial Ald is composed of six identical subunits with the N-terminal catalytic and C-terminal

Received 14 March 2018 **Accepted** 25 April 2018

Accepted manuscript posted online 30 April 2018

Citation Jeong J-A, Park SW, Yoon D, Kim S, Kang H-Y, Oh J-I. 2018. Roles of alanine dehydrogenase and induction of its gene in *Mycobacterium smegmatis* under respiration-inhibitory conditions. J Bacteriol 200:e00152-18. https://doi.org/10.1128/JB.00152-18.

Editor William W. Metcalf, University of Illinois at Urbana Champaign

Address correspondence to Jeong-Il Oh, joh@pusan.ac.kr.

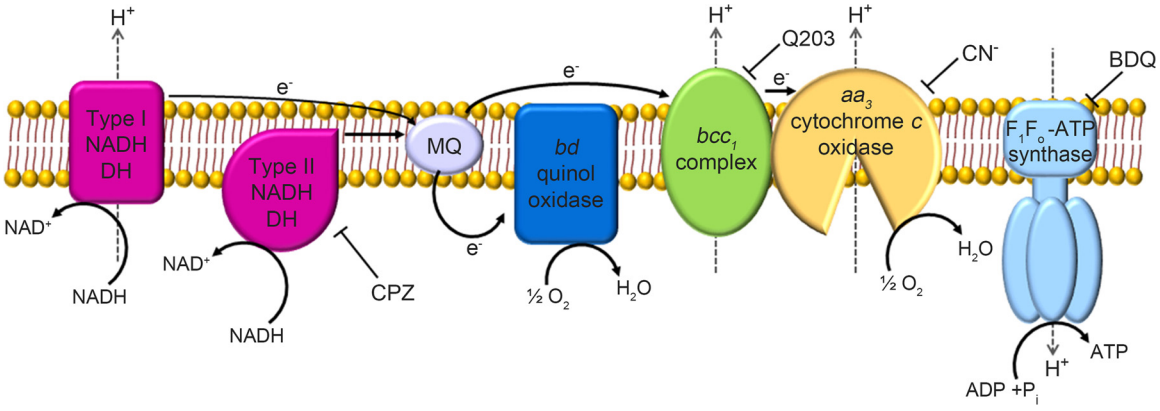

FIG 1 The respiratory electron transport chain of *M. smegmatis*. Electron flow is indicated by the solid arrows. The dashed arrows indicate the translocation of protons across the membrane. Abbreviations: DH, dehydrogenase; MQ, menaquinone pool; CN^-, cyanide; CPZ, chlorpromazine; BDQ, bedaquiline.

NAD(H)-binding domains (8, 9). It has been reported that Ald is one of the major antigens found in culture filtrates of *M. tuberculosis* (10, 11).

The expression of the *ald* gene was strongly upregulated in *M. tuberculosis* and *M. smegmatis* grown in the presence of alanine (2, 3, 12, 13). This alanine-dependent regulation of *ald* was shown to be mediated by the AldR transcriptional regulator that belongs to the Lrp/AsnC (leucine-responsive regulatory protein/asparagine synthase C) family (12, 13). Furthermore, the expression of the *ald* gene was shown to be upregulated in *M. smegmatis* under hypoxic conditions, which is independent of the DevSR (DosSR) two-component system that is the major regulatory system involved in oxygen and NO sensing in mycobacteria (12). Other studies also reported that the expression of the *ald* gene, as well as the activity and synthesis of Ald, was increased in *M. tuberculosis* and *M. smegmatis* grown under oxygen-limiting conditions (2, 3, 5–7, 14–16). The expression of the *ald* gene was shown to be upregulated in *M. tuberculosis* grown under nutrient starvation conditions and in *Mycobacterium marinum* during its persistence in granulomas (4, 17). The treatment of *M. smegmatis* cultures with bedaquiline (BDQ), which inhibits the F_1F_o-ATP synthase by binding to c subunits, reportedly led to the induction of *ald* expression (18).

The redox balance of NADH/NAD^+ is influenced by oxygen availability and the functionality of the electron transport chain (ETC) (19–21). *M. smegmatis* contains the branched respiratory ETC, which is terminated with two terminal oxidases (Fig. 1). One branch consists of the cytochrome bcc_1 complex and aa_3 cytochrome *c* oxidase, while the other is terminated with the *bd* quinol oxidase. The aa_3 cytochrome *c* oxidase forms a supercomplex with the cytochrome bcc_1 complex (22). Since the aa_3 cytochrome *c* oxidase is the major terminal oxidase in *M. smegmatis* grown aerobically, the bcc_1-aa_3 branch is required for the optimal growth of *M. smegmatis* under aerobic conditions, and its disruption results in some growth retardation and upregulation of the *bd* quinol oxidase genes (23, 24). The *bd* quinol oxidase was shown to have a high affinity for oxygen, thereby being considered to play a crucial role under oxygen-limiting conditions (23, 24). There are two NADH dehydrogenases (type I and type II) that are linked to the ETC in mycobacteria. Several studies have suggested that the non-proton-translocating type II NADH dehydrogenase encoded by *ndh* in *M. tuberculosis* and *M. smegmatis* is the major NADH dehydrogenase responsible for recycling NADH to NAD^+ during aerobic respiration (25–29). In addition to *ndh*, *M. tuberculosis* possesses the *ndhA* gene, annotated as a type II NADH dehydrogenase gene, which does not occur in *M. smegmatis* (25, 30, 31).

We previously hypothesized that the hypoxic induction of *ald* might be caused by increased levels of alanine in *M. smegmatis* grown under hypoxic conditions (12). However, the precise induction mechanism of the *ald* gene under hypoxic conditions

remains unclarified. In this study, we present several lines of evidence indicating that the extent of electron flux through the ETC determines the expression level of the *ald* gene by affecting the intracellular level of alanine. Comparative analyses of growth of *M. smegmatis* strains treated with ETC inhibitors revealed that Ald is instrumental in the survival of the mycobacterium under severe respiration-inhibitory conditions by maintaining redox homeostasis of NADH/NAD^+.

RESULTS

Respiration rates of the terminal oxidase mutant strains of *M. smegmatis*. Our previous study demonstrated that the expression of *ald* is induced in *M. smegmatis* under hypoxic conditions independently of the DevSR two-component system (12). A possible mechanism for the hypoxic induction of *ald* is that the inhibition of electron flux through the ETC under oxygen-limiting conditions is associated with the induction of *ald* expression. To assess this possibility, two terminal oxidase mutant (Δ*bd* and Δaa_3) strains of *M. smegmatis* were constructed. No difference in the growth rate between the wild-type (WT) and Δ*bd* mutant strains of *M. smegmatis* was observed under aerobic conditions (data not shown). However, the growth of the Δaa_3 mutant was slower and reached the stationary phase at a lower cell density than that of the WT (the doubling times of the WT and Δaa_3 mutant are 5.1 and 6.9 h, respectively).

To examine to what extent electron flux through the respiratory ETC is inhibited in the two terminal oxidase mutants of *M. smegmatis*, the rate of oxygen consumption was measured using membrane fractions of the WT and two mutant strains grown aerobically (Fig. 2A). Oxygen consumption did not occur in the absence of added NADH as an electron donor (data not shown). When NADH was added, the Δaa_3 and Δ*bd* mutant strains exhibited 53.1 and 85.8% of the oxygen consumption rate observed for the WT, respectively.

We determined the expression level of the *cydA* gene encoding subunit I of the *bd* quinol oxidase in the WT and terminal oxidase mutant strains by reverse transcription-PCR (RT-PCR) and quantitative real-time PCR (qRT-PCR) (Fig. 2B). The transcript levels of *cydA* in the Δaa_3 mutant grown aerobically and in the WT strain grown under hypoxic conditions were increased by 6.4-fold and 16.3-fold, respectively, compared to that in the WT grown aerobically. We also examined the expression level of the *ctaC* gene encoding subunit II of the aa_3 cytochrome *c* oxidase. The expression level of *ctaC* in the Δ*bd* and Δaa_3 mutants grown aerobically was almost same as that in the control WT grown aerobically. However, the expression of *ctaC* in the WT strain grown under hypoxic conditions was rather decreased compared to that in the WT strain grown aerobically. Altogether, these results confirm the previous findings (23, 24, 32), that the aa_3 cytochrome *c* oxidase is the major terminal oxidase in the respiratory ETC of *M. smegmatis* grown aerobically and that inhibition of the ETC by the depletion of oxygen or inactivation of the bcc_1-aa_3 branch leads to the shift of terminal oxidases from the aa_3 cytochrome *c* oxidase to the *bd* quinol oxidase in *M. smegmatis*.

Effect of respiration inhibition on *ald* expression. The effect of ETC inhibition on *ald* expression was investigated by determining the promoter activity of *ald* in the WT and Δaa_3 mutant strains grown aerobically, as well as in the WT strain grown under hypoxic conditions for 20 h (Fig. 2C). Since the Δaa_3 mutant showed 53% of the respiration rate observed for the WT strain (Fig. 2A), the expression level of *ald* in the Δaa_3 mutant is likely to represent that in the WT strain when its respiratory ETC is inhibited by approximately 50%. The WT and Δaa_3 mutant strains used in this experiment harbored an *ald*::*lacZ* transcriptional fusion plasmid, pALDLACZ. The aerobically grown Δaa_3 mutant of *M. smegmatis* with the empty integration vector pMV306 showed a 12.5-fold increase in *ald* expression compared to that in the WT strain containing pMV306 grown under the same conditions. The expression level of *ald* in the Δaa_3 mutant was restored to that in the WT by the introduction of pMV306ctaC containing the intact *ctaC* gene into the Δaa_3 mutant, indicating that the induction of *ald* expression observed for the Δaa_3 mutant resulted from the disruption of the *ctaC* gene. The expression of *ald* in the WT strain grown under hypoxic conditions was

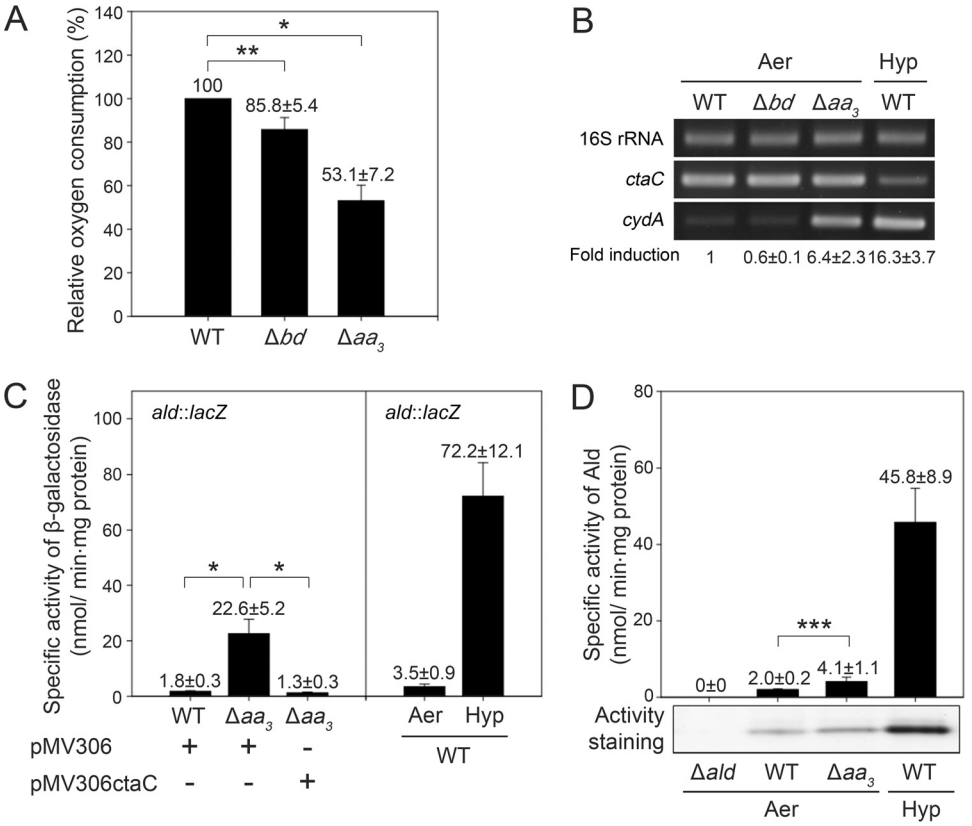

FIG 2 Respiration rates of the terminal oxidase mutant (Δ*bd* and Δaa_3) strains and effects of respiration inhibition by inactivation of the aa_3 oxidase or hypoxic cultivation on *ald* expression in *M. smegmatis*. *M. smegmatis* strains were grown either aerobically to an OD_{600} of 0.7 to 0.8 (Aer) or under hypoxic conditions (Hyp) for 20 h. (A) Oxygen consumption rates of the terminal oxidase mutant strains were determined using membrane fractions of the *M. smegmatis* strains grown aerobically. The oxygen consumption rate of the WT strain is set at 100, and relative rates are expressed for the other strains. All values provided are the averages of the results from three independent determinations. (B) Expression of terminal oxidase genes in the terminal oxidase mutant strains of *M. smegmatis*. Expression levels of *ctaC*, *cydA*, and 16S rRNA genes were determined by RT-PCR. RT-PCR for 16S rRNA was conducted to ensure that the same amounts of total RNA were employed for RT-PCR. The level of *cydA* mRNA was quantitatively determined by qRT-PCR. Fold induction of *cydA* expression indicates the level of *cydA* mRNA relative to that in the WT cells grown under aerobic conditions and is given below the RT-PCR results. The fold induction values provided are the averages of the results from two independent determinations. (C) Expression levels of *ald* in the WT and Δaa_3 strains grown aerobically, as well as in the WT strain grown under hypoxic conditions, were determined using an *ald*::*lacZ* transcriptional fusion plasmid, pALDLACZ. To compare the expression level of *ald* in the Δaa_3 mutant with that in the WT strain, the aerobically grown WT and Δaa_3 mutant strains carrying the empty vector pMV306 were used in the experiment. For complementation of the Δaa_3 mutant, pMV306ctaC carrying the intact *ctaC* gene was introduced into the mutant. All values provided are the averages of the results from four independent determinations. (D) The specific activity and activity staining of Ald in the WT and Δaa_3 mutant strains grown aerobically or under hypoxic conditions. The Δ*ald* mutant strain without Ald activity was included in the experiment as a negative control. All values provided are the averages of results from three independent determinations. Crude extracts (20 μg) were subjected to nondenaturing PAGE on a 7.5% (wt/vol) acrylamide gel, and the gel was subsequently stained by Ald activity. *, $P < 0.01$; **, $P < 0.05$; ***, $P < 0.1$.

20.6-fold higher than that detected in the same strain grown aerobically. The expression of *ald* in the *M. smegmatis* strains was also determined at the protein level by both measuring Ald activity and performing activity staining of Ald (Fig. 2D). The Δ*ald* mutant strain was included in the experiment as a negative control. The specific activities of Ald were 2.1-fold and 22.9-fold higher in the Δaa_3 mutant grown aerobically and the WT strain grown under hypoxic conditions, respectively, than in the control WT grown aerobically. The level of the active Ald protein determined by activity staining correlated well with the determined Ald activity (Fig. 2D).

The expression of the *ald* gene in *M. smegmatis* has been demonstrated to be under the control of the AldR transcriptional regulator that senses the intracellular level of alanine (12, 13). To investigate whether the hypoxic induction of *ald* is mediated by

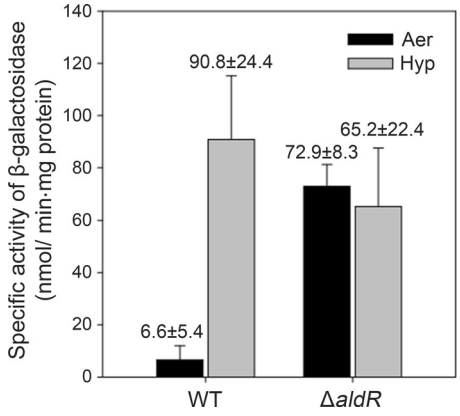

FIG 3 Expression of the *ald* gene in the WT and Δ*aldR* mutant strains of *M. smegmatis*. The WT and Δ*aldR* mutant strains of *M. smegmatis* carrying the *ald*::*lacZ* transcriptional fusion plasmid (pALDLACZ) were grown either aerobically to an OD_{600} of 0.5 to 0.6 (Aer) or under hypoxic conditions (Hyp) for 20 h. The *ald* promoter activities were measured by determining β-galactosidase activity. All values provided are the averages of the results from three independent determinations. Error bars indicate the standard deviations.

AldR in *M. smegmatis*, we determined the promoter activity of *ald* in the WT and Δ*aldR* mutant strains grown either aerobically (Aer) or under hypoxic conditions for 20 h (Hyp) by using pALDLACZ (Fig. 3). In agreement with our previous results (12, 13), *ald* expression was partially derepressed in the Δ*aldR* mutant grown aerobically relative to that in the WT strain grown under the same conditions. The expression of *ald* was not induced in the Δ*aldR* mutant grown under hypoxic conditions, while the hypoxic induction of *ald* occurred in the WT strain. These results indicate that the hypoxic induction of *ald* expression is mediated by AldR.

We next examined the effect of cyanide, which is an inhibitor of the aa_3 cytochrome *c* oxidase, on *ald* expression in the WT and Δ*aldR* mutant strains of *M. smegmatis* grown aerobically. The expression level of the *ald* gene was determined by RT-PCR and qRT-PCR (Fig. 4). We could not use an *ald*::*lacZ* transcriptional fusion to determine the expression level of *ald* in this experiment, since the addition of KCN interfered with the expression of β-galactosidase for unknown reasons (33). The expression of *ald* was increased in the WT strain in proportion to the concentration of KCN and reached a maximum level at 50 μM KCN (Fig. 4A), while the expression of *ald* was not induced by KCN treatment in the Δ*aldR* mutant strain (Fig. 4B). Altogether, these results indicate that the inhibition of electron flux through the ETC by inactivation of the aa_3 cytochrome *c* oxidase or by limitation of oxygen availability results in the induction of *ald* expression in an AldR-dependent way.

Finally, the effect of cyanide on *ald* expression in the WT and Δ*bd* mutant strains grown aerobically was examined (Fig. 5). The expression level of the *ald* gene was determined by RT-PCR. Since the *bd* quinol oxidase is known to be insensitive to cyanide in contrast to the aa_3 cytochrome *c* oxidase, we expected that the ETC of the Δ*bd* mutant expressing only the aa_3 cytochrome *c* oxidase as a terminal oxidase would be more severely inhibited by cyanide than that of the WT strain expressing both the *bd* quinol oxidase and aa_3 cytochrome *c* oxidase. The expression levels of *ald* in both strains were increased with increasing concentrations of KCN. Interestingly, the expression of *ald* in the Δ*bd* mutant was more induced in the low concentration range of KCN (10 and 20 μM) than that detected in the WT strain, confirming the inverse relationship between the extent of electron flux through the ETC and *ald* expression.

Redox state of pyridine nucleotides and intracellular concentrations of alanine in *M. smegmatis* under respiration-inhibitory conditions. Since NADH produced by catabolic reactions acts as a major electron donor for the ETC, we assumed that the inhibition of the ETC by either disruption of the aa_3 cytochrome *c* oxidase or depletion of oxygen shifts the redox state of the NADH/NAD^+ pool to a more reduced state in the

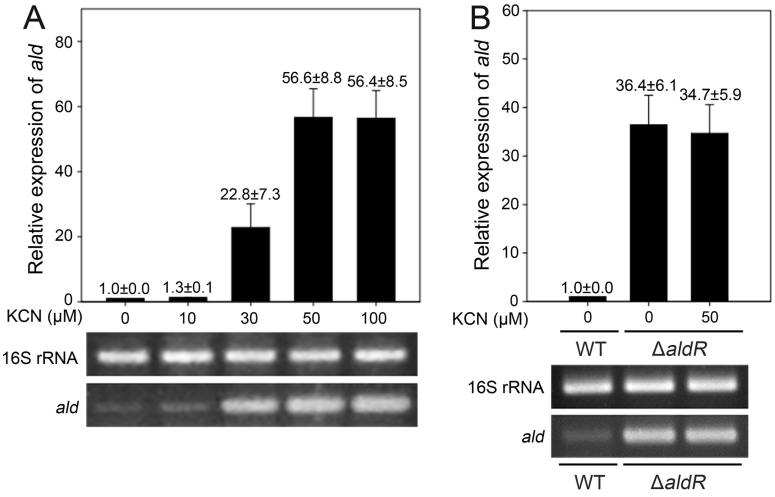

FIG 4 Effect of respiration inhibition by KCN on *ald* expression in the WT (A) and Δ*aldR* mutant (B) strains of *M. smegmatis* grown under aerobic conditions. The WT and Δ*aldR* mutant strains of *M. smegmatis* were grown aerobically in 7H9-glucose medium to an OD_{600} of 0.5 to 0.6. Following the addition of the given concentrations of KCN to the cultures, the strains were further grown for 15 min. As controls, the WT and Δ*aldR* mutant strains were grown aerobically without KCN treatment. Expression levels of *ald* were determined by qRT-PCR and RT-PCR. The transcript level of *ald* determined by qRT-PCR was normalized to that of 16S rRNA. The relative level of *ald* expression indicates the level of *ald* mRNA in the WT (A) or Δ*aldR* mutant (B) strains treated with KCN relative to that in the untreated WT strain (0 μM). All values provided are the averages of the results from two independent determinations. Error bars indicate the deviations from the means.

cell. To confirm this assumption, we determined the redox state of the pyridine nucleotide pool in the WT and Δaa_3 mutant strains grown aerobically, as well as in the WT grown under hypoxic conditions (Fig. 6). The total amounts of pyridine nucleotides (NADH plus NAD^+) in the *M. smegmatis* strains ranged from 959.5 to 1,478.1 pmol/ml. When the WT strain was grown under hypoxic conditions for 20 h, the NADH/NAD^+ ratio was increased by approximately 2-fold relative to that determined in the control WT strain grown aerobically. A 1.43-fold increase in the NADH/NAD^+ ratio was observed in the Δaa_3 mutant grown aerobically compared to that in the WT strain grown aerobically. These findings indicate that the blockage of electron flow through the ETC might exert back pressure on the ETC, thereby diminishing the rate of NADH oxidation and shifting the redox balance of NADH/NAD^+ toward a more reduced state.

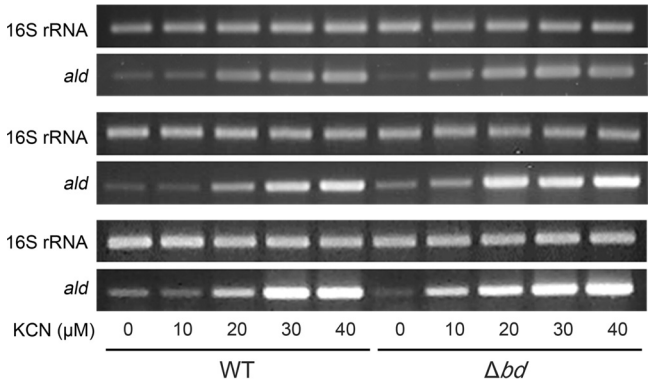

FIG 5 Comparison of *ald* expression between the WT and Δ*bd* mutant strains of *M. smegmatis* treated with increasing concentrations of KCN. The WT and Δ*bd* mutant strains were grown as described for Fig. 4. Expression levels of *ald* and 16S rRNA genes were determined by RT-PCR. RT-PCR for 16S rRNA was conducted to ensure that the same amounts of total RNA were employed for RT-PCR. RT-PCR was performed in triplicates using total RNA isolated from three independent cultures of the WT and Δ*bd* mutant strains.

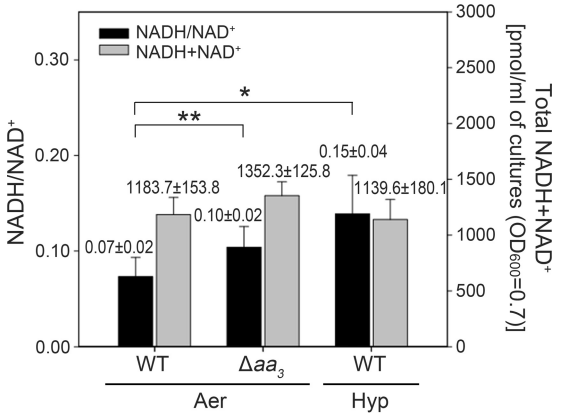

FIG 6 Effect of respiration inhibition on intracellular levels of total pyridine dinucleotides (NADH+NAD$^+$) and the NADH/NAD$^+$ ratio in the WT and Δ*aa*$_3$ mutant strains of *M. smegmatis*. *M. smegmatis* strains were grown either aerobically to an OD_{600} of 0.7 to 0.8 (Aer) or under hypoxic conditions (Hyp) for 20 h. All values provided are the averages from seven independent determinations. Error bars indicate the standard deviations. *, $P < 0.01$; **, $P < 0.05$.

The maintenance of redox homeostasis is essential for the survival and growth of mycobacteria. Therefore, we reasoned that the high ratio of NADH to NAD$^+$ under respiration-inhibitory conditions might trigger the reductive amination reaction by Ald, converting pyruvate to alanine with the concomitant oxidation of NADH to NAD$^+$ to maintain redox balance in a similar way as lactate fermentation. An increase in alanine concentrations in turn induces *ald* expression through the alanine-responsive AldR regulator (12, 13). To test this hypothesis, the intracellular levels of alanine in the WT strain of *M. smegmatis* grown aerobically and under hypoxic conditions, as well as in the Δ*aa*$_3$ mutant grown aerobically, were determined by means of nuclear magnetic resonance (NMR) analysis. As shown in Fig. 7 (representative NMR spectra are shown in Fig. S1 in the supplemental material), the intracellular level of alanine in the Δ*aa*$_3$ mutant grown aerobically was increased by 1.7-fold relative to that in the WT strain

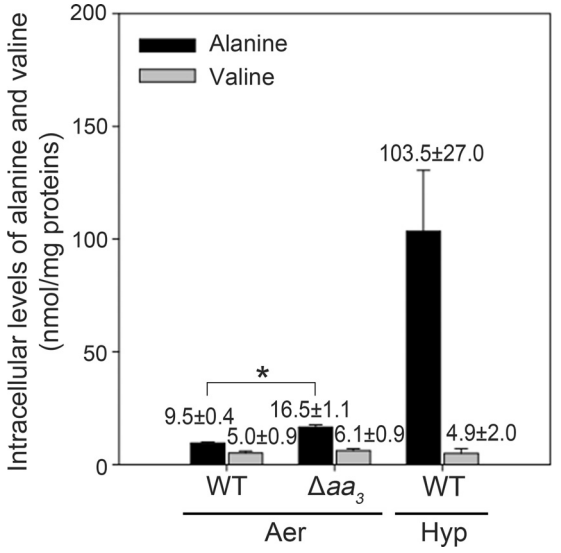

FIG 7 Determination of intracellular concentrations of alanine and valine. The WT and Δ*aa*$_3$ mutant strains were grown either aerobically to an OD_{600} of 0.7 to 0.8 (Aer) or under hypoxic conditions (Hyp) for 20 h. Cell-free crude extracts containing 4 mg of proteins were subjected to methanol-chloroform extraction and the obtained aqueous phase was used for ^{1}H-NMR analysis to determine the amounts of alanine and valine. Intracellular levels of alanine and valine are expressed as nmol/mg of proteins. All values provided are the averages from three independent determinations. Error bars indicate the standard deviations. *, $P < 0.001$.

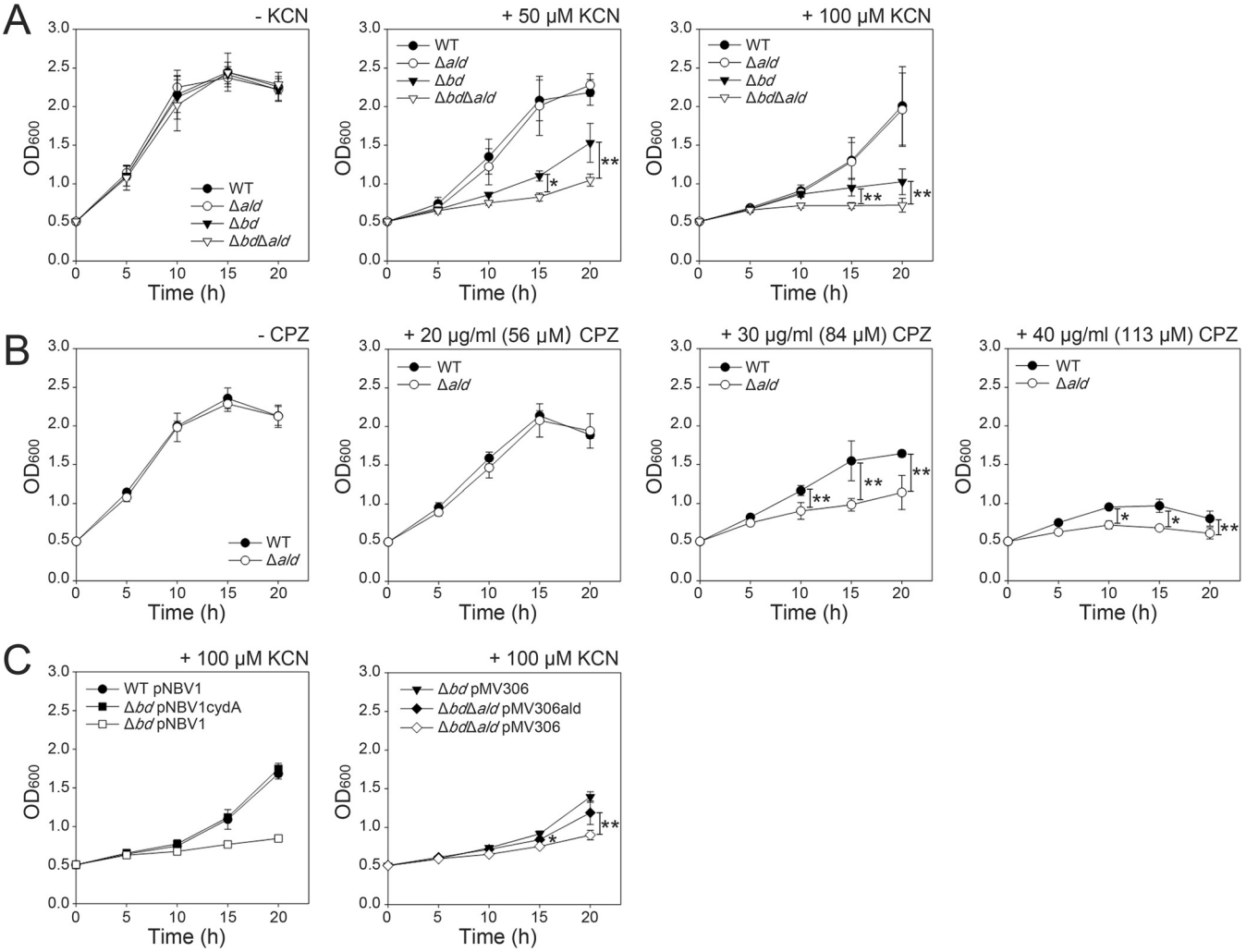

FIG 8 Effect of respiration inhibitors (KCN and CPZ) on aerobic growth of the WT and mutant (Δ*ald*, Δ*bd*, and Δ*bd* Δ*ald*) strains of *M. smegmatis*. *M. smegmatis* strains were grown aerobically in 7H9-glucose medium to an OD_{600} of 0.5, and cyanide (A and C) or CPZ (B) was added to the cultures to the given concentrations. The cultures were further grown for 20 h, and the growth of the strains was monitored spectrophotometrically at 600 nm at 5-h intervals. (C) For complementation tests, pNBV1cydA and pMV306ald, which carry the intact *cydA* and *ald* genes, respectively, were used to complement the Δ*bd* and Δ*bd* Δ*ald* mutant strains. As controls, the *M. smegmatis* strains with the empty vector, pNBV1 or pMV306, were included in the experiment. All values provided are the averages of the results from three independent determinations. Error bars indicate the standard deviations. *, $P < 0.01$; **, $P < 0.05$.

grown aerobically. When grown under hypoxic conditions (Hyp), the WT strain produced a 10.9-fold higher level of alanine than the control WT strain grown aerobically. The intracellular levels of valine in the same strains were measured in the experiment as a reference. No significant differences in valine levels were observed between the strains tested. The intracellular levels of alanine in the *M. smegmatis* strains correlated well with the expression levels of *ald* in the same strains (Fig. 2). These results suggest that the intracellular levels of alanine reflect the functional state of the ETC and that the induction of *ald* expression under respiration-inhibitory conditions is a consequence of increased intracellular alanine levels.

Ald is required for optimal growth of *M. smegmatis* under severe respiration-inhibitory conditions. To ascertain the role of Ald in the growth of *M. smegmatis* under ETC inhibition, we comparatively examined the growth of the *M. smegmatis* strains (WT, Δ*bd*, Δ*ald*, and Δ*bd* Δ*ald* mutant strains) in the presence of KCN and chlorpromazine (CPZ), which are inhibitors of the aa_3 cytochrome *c* oxidase and type II NADH dehydrogenase, respectively. As shown in Fig. 8A, all mutant strains grew on 7H9-glucose medium without KCN treatment at approximately the same rate as the WT strain. When

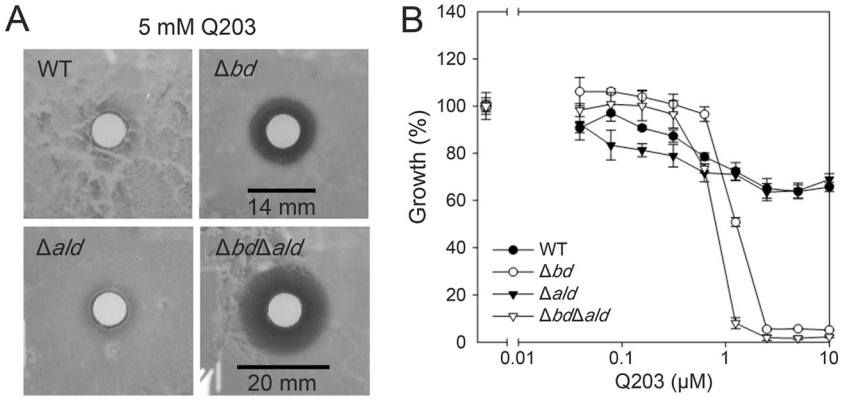

Strain	MIC_{50} (μM)	MIC_{90} (μM)
WT	> 10	> 10
Δ*bd*	1.26±0.04	2.10±0.08
Δ*ald*	> 10	> 10
Δ*bd*Δ*ald*	0.77±0.02*	1.20±0.09*

FIG 9 Susceptibility of the WT and mutant (Δ*bd*, Δ*ald*, and Δ*bd* Δ*ald*) strains of *M. smegmatis* to Q203. (A) Zone inhibition assay. (B) MIC of Q203 for the WT and mutant strains. Log-transformed Q203 concentrations were plotted against the growth of the strains normalized to that of Q203-untreated cultures. The MIC_{50} and MIC_{90} values of Q203 for the WT and mutant strains of *M. smegmatis* are presented in the table below the plot. All values provided are the averages of the results from three independent determinations. Error bars indicate the standard deviations. *, $P < 0.001$ between the Δ*bd* and Δ*bd* Δ*ald* mutant strains.

M. smegmatis cultures were treated with 50 and 100 μM KCN, the growth of the Δ*bd* mutant was significantly retarded relative to that of the WT strain, which is in agreement with the previous report suggesting that the *bd* quinol oxidase is a CN^--insensitive terminal oxidase and plays an important role in aerobic respiration in the case of aa_3 oxidase inhibition (23). The expression of the intact *cydA* gene from a multicopy plasmid, pNBV1cydA, completely restored the growth rate of the Δ*bd* mutant to that of the WT strain (Fig. 8C). Intriguingly, the treatment with KCN resulted in a more severe growth defect for the Δ*bd* Δ*ald* double mutant than for the Δ*bd* mutant, while the Δ*ald* mutant and the WT strains showed no difference in growth in the presence of KCN. When *ald* was expressed from an integration plasmid, pMV306ald, the impaired growth of the Δ*bd* Δ*ald* double mutant was partially recovered to the Δ*bd* mutant level (Fig. 8C). The partial complementation of the Δ*bd* Δ*ald* mutant by pMV306ald might result from insufficient expression of the integrated *ald* gene.

Type II NADH dehydrogenase, which donates electrons from NADH to the ETC without proton translocation across the membrane, is known to be the major NADH dehydrogenase in mycobacteria (25, 28–30, 34). When the WT and Δ*ald* mutant strains were grown in the presence of CPZ, their growth was more inhibited with increasing concentrations of CPZ (Fig. 8B). The inactivation of *ald* negatively affected the growth of *M. smegmatis* at CPZ concentrations (30 and 40 μg/ml) where the growth of the WT strain was inhibited.

We next examined the susceptibility of the *M. smegmatis* strains (WT, Δ*bd*, Δ*ald*, and Δ*bd* Δ*ald* mutant strains) to Q203, which specifically inhibits the cytochrome bcc_1 complex by binding to the cytochrome *b* subunit (QcrB) (35), by performing a zone inhibition assay (Fig. 9A). No zone of inhibition was observed for the WT and Δ*ald* mutant strains when 20 μl of 5 mM Q203 was used. In contrast, the Δ*bd* mutant exhibited a susceptibility to Q203 as indicated by the formation of a clear zone (14-mm diameter) around the disc. The Δ*bd* Δ*ald* mutant gave rise to a larger clear zone (20-mm diameter) than the Δ*bd* mutant, indicating that the Δ*bd* Δ*ald* mutant is more susceptible to Q203 than the Δ*bd* mutant. To define the inhibitory activity of Q203 quantitatively, the MIC_{50} and MIC_{90} values of Q203 were determined for the WT and mutant strains of *M. smegmatis* (Fig. 9B). In agreement with

the results of the zone inhibition assay, the MIC_{50} and MIC_{90} values of Q203 for the WT and Δ*ald* mutant strains of *M. smegmatis* were greater than 10 μM. The MIC_{50} (1.26 μM) and MIC_{90} (2.10 μM) values of Q203 for the Δ*bd* mutant were much lower than those for the WT and Δ*ald* mutant strains. The inactivation of the *ald* gene in the Δ*bd* mutant (Δ*bd* Δ*ald* mutant) further decreased the MIC_{50} and MIC_{90} of Q203. Taken together, the results presented in Fig. 8 and 9 imply that Ald is of benefit to *M. smegmatis* under severe respiration-inhibitory conditions, probably by maintaining the redox balance of NADH/NAD^+.

DISCUSSION

Induction of *ald* expression under respiration-inhibitory conditions. Alanine availability was shown to be a major determinant for the induction of *ald* expression in *M. smegmatis* (12, 13). The addition of alanine to aerobic cultures of *M. smegmatis* and *M. tuberculosis* was shown to result in a strong induction of *ald* expression (2, 3, 12, 13). This alanine-responsive upregulation of *ald* is mediated by the AldR transcriptional regulator that uses alanine as an effector molecule (12, 13). An interesting aspect regarding *ald* expression is the hypoxic induction of *ald* in *M. smegmatis* independently of the DevSR two-component system (12). The clue as to how *ald* expression is induced under hypoxic conditions emerged from the following findings: the treatment of *M. smegmatis* cultures with BDQ, which is an inhibitor of the mycobacterial F_1F_o-ATP synthase and therefore also inhibits the mycobacterial ETC, led to the induction of *ald* expression (18). The intracellular levels of alanine and glycine were increased in *M. tuberculosis* exposed to hypoxic conditions (21).

Since dioxygen is a final electron acceptor of the ETC during aerobic respiration, electron flux through the ETC is expected to be inhibited under oxygen-limiting conditions. Therefore, it is possible that the hypoxic induction of *ald* in *M. smegmatis* is mediated by AldR in response to the elevated intracellular level of alanine under respiration-inhibitory conditions. As conclusive proof that the reduced functionality of the ETC, rather than the direct regulation of *ald* by an O_2-sensing regulatory system, pertains to the hypoxic induction of *ald* expression, we demonstrated that the inhibition of electron flux through the ETC by either the inactivation of the aa_3 cytochrome *c* oxidase or treatment of *M. smegmatis* cultures with KCN under aerobic conditions resulted in the induction of *ald* expression (Fig. 2 and 4). The expression level of *ald* in *M. smegmatis* grown aerobically was proportional to the concentration of used KCN, and the induction effect of KCN was more prominent in the Δ*bd* mutant strain of *M. smegmatis* than in the WT strain (Fig. 5), which strongly implies that the extent of *ald* expression is inversely related to the functionality of the ETC.

We showed that the reduction in functionality of the ETC and oxygen availability led to an increase in the NADH/NAD^+ ratio in *M. smegmatis* (Fig. 6). Consistent with our result, it has been reported that the NADH/NAD^+ ratio was increased in *M. tuberculosis* treated with ETC inhibitors, as well as in *M. tuberculosis* either residing within macrophages or grown under oxygen-limiting conditions (20, 21, 36–39). When glucose is supplied to mycobacteria as a carbon source under respiration-inhibitory conditions, pyruvate (the final product of glycolysis) is not efficiently catabolized to CO_2 through the tricarboxylic acid (TCA) cycle due to NAD^+ insufficiency. When the pyruvate level and NADH/NAD^+ ratio are elevated, the reaction rate for the reductive amination of pyruvate to alanine with the concomitant oxidation of NADH to NAD^+ is assumed to be accelerated because of the elevated level of substrates, which accounts for an increase in the intracellular level of alanine in *M. smegmatis* under respiration-inhibitory conditions (under hypoxic conditions and in the Δaa_3 mutant) (Fig. 7). Furthermore, our study showed that the expression level of *ald* correlates well with the intracellular level of alanine in *M. smegmatis* (Fig. 2 and 7) and that the induction of *ald* expression under respiration-inhibitory conditions is dependent on AldR (Fig. 3 and 4B). These findings suggest that alanine is the direct effector molecule for the induction of *ald* expression under respiration-inhibitory conditions and that the intracellular level of alanine indirectly reflects the functional state of the ETC.

On the basis of the results presented here, we suggest a model explaining the induction of *ald* expression in response to respiration inhibition. The exposure of mycobacteria to respiration-inhibitory conditions leads to the inhibition of electron flow through the respiratory ETC. Reduced functionality of the ETC shifts the redox state of the NADH/NAD^+ pool to a more reduced state, exerting a negative effect on NADH-producing metabolic pathways such as pyruvate oxidation and the oxidative TCA cycle. The increased levels of NADH and pyruvate in cells most likely promote the synthesis of alanine from pyruvate through the reductive amination reaction by Ald. As a result, the intracellular concentration of alanine is increased, which in turn induces the expression of the *ald* gene through AldR.

Roles of Ald in mycobacterial survival under severe respiration-inhibitory conditions. We demonstrated that the Δ*bd* Δ*ald* double mutant of *M. smegmatis* was more susceptible to KCN and Q203 than the Δ*bd* mutant, while the WT and Δ*ald* mutant strains of *M. smegmatis* did not show noticeable differences in their susceptibility to KCN and Q203 (Fig. 8A and 9). The treatment of growth cultures with CPZ resulted in more severe growth inhibition for the Δ*ald* mutant than for the WT strain (Fig. 8B). On the basis of these results, we assumed that Ald plays an important role in the growth and survival of *M. smegmatis* under severe respiration-inhibitory conditions such as hypoxic or inhibitory conditions of both the bcc_1-aa_3 branch and *bd* quinol oxidase. In good agreement with these results, an *ald* mutant of *M. smegmatis* reportedly displayed a decreased survival rate under oxygen depletion conditions compared to that of the WT strain grown under the same conditions (3). The reoxidation of NADH by Ald seems likely to play a pivotal role in the redox homeostasis of NADH/NAD^+ when mycobacteria are confronted with severe respiration-inhibitory conditions under which the ETC does not function sufficiently to maintain the redox homeostasis of NADH/NAD^+. In this respect, the reductive amination of pyruvate to alanine by Ald is reminiscent of the reduction of pyruvate to lactate by lactate dehydrogenase in lactate fermentation. A search for the lactate dehydrogenase gene in the *M. smegmatis* genome led us to conclude that *M. smegmatis* does not possess NADH/NAD^+-dependent lactate dehydrogenase. Therefore, we assume that Ald might play a similar role as lactate dehydrogenase when *M. smegmatis* utilizes glucose under respiration-inhibitory conditions. It has been reported that the impaired anaerobic growth of a lactate dehydrogenase (*ldh*) mutant strain of *Escherichia coli* could be recovered by complementation with *M. tuberculosis ald* (6), which supports our assumption. Using this metabolic pathway similar to "alanine fermentation," *M. smegmatis* can theoretically generate two molecules of ATP per one molecule of glucose by substrate-level phosphorylation while maintaining the redox homeostasis of NADH/NAD^+. Furthermore, the rapid consumption of pyruvate through alanine fermentation by Ald can reduce the accumulation of glycolytic intermediates, which is known to be toxic to *M. tuberculosis* under hypoxic conditions (40). It has been suggested that the reductive branch of the TCA cycle and the glyoxylate shunt from the TCA cycle participate in both the reoxidation of reducing equivalents and the supply of biosynthetic precursors under respiration-inhibitory conditions (6, 19, 21, 38). Since Ald also has glycine dehydrogenase activity that catalyzes the reductive amination of glyoxylate to glycine, this activity is also expected to contribute to the reoxidation of NADH in the glyoxylate shunt (2, 7).

It has been demonstrated that *Mycobacterium bovis* bacillus Calmette-Guérin (BCG) is more vulnerable to bcc_1 inhibitors than *M. tuberculosis* (41). The MIC_{90} values of imidazo[1,2-α]pyrimidine and imidazo[1,2-α]pyridine amide (IPA) derivatives for *M. bovis* BCG were lower than those for *M. tuberculosis* (41). Although the nucleotide sequences of the *M. tuberculosis* and *M. bovis* BCG genomes exhibit 99.95% overall identity (42), Ald of *M. bovis* BCG is functionally inactive due to a frameshift mutation within its gene (1), which might be the reason for the higher susceptibility of *M. bovis* BCG to the bcc_1 complex inhibitors than of *M. tuberculosis*. Ald has long been recognized as a potential virulence factor. Therefore, small-molecule inhibitors targeting Ald

have been developed (43, 44). On the basis of our findings together with the aforementioned reports, we suggest that combinatory therapeutic regimens including both an Ald-specific inhibitor and respiration-inhibitory antitubercular drugs like Q203 and BDQ are likely to act against *M. tuberculosis* more efficiently than single-drug regimens.

Speculation on the mechanism underlying resistance of *M. smegmatis* to bcc_1 complex inhibitors. Our results (Fig. 9) and those reported previously (18, 41, 45–49) showed that *bd* quinol oxidase mutants of *M. smegmatis* and *M. tuberculosis* are more susceptible to bcc_1 complex inhibitors and BDQ than the corresponding isogenic WT strains, which indicates the requirement of the *bd* quinol oxidase for aerobic respiration of the mycobacteria when the bcc_1-aa_3 branch of the ETC is inactivated. *M. tuberculosis* is known to be much more sensitive to bcc_1 complex inhibitors such as Q203 and lansoprazole than *M. smegmatis* (35, 41, 50). The MIC_{50} of Q203 and the MIC_{90} of lansoprazole for *M. tuberculosis* were reported to be 2.7 nM and 1.13 μM, respectively, while the MIC_{90} values of Q203 and lansoprazole for *M. smegmatis* were reported to be $>$20 μM and $>$100 μM, respectively (35, 50). From these findings, we assumed that the resistance of *M. smegmatis* to bcc_1 complex inhibitors might be, at least in part, attributable to the high expression levels of the *bd* quinol oxidase in *M. smegmatis* exposed to the inhibitory conditions of the bcc_1-aa_3 branch. In good agreement with our assumption, the result presented in Fig. 2 revealed that the expression of the *cydAB* operon is strongly upregulated in the Δaa_3 mutant of *M. smegmatis* and that the mutant still retains as much as half of the respiration capability of the WT. The construction of the bcc_1 complex and aa_3 cytochrome *c* oxidase mutants of *M. tuberculosis* was reportedly unsuccessful in contrast to that for *M. smegmatis*, for which the mutants were successfully generated (24, 26, 45, 51). The indispensability of the bcc_1-aa_3 branch of the ETC for *M. tuberculosis* implies that the expression level of the *bd* quinol oxidase in *M. tuberculosis* might not be sufficient to compensate for the inactivation of the bcc_1-aa_3 branch, which provides a strong rationale for the high susceptibility of *M. tuberculosis* to bcc_1 complex inhibitors in contrast to that of *M. smegmatis*.

In summary, we demonstrated that the regulation of *ald* expression in *M. smegmatis* is closely associated with the functionality of the respiratory ETC. Together with AldR, the ETC constitutes a signal transduction system in which alanine serves as a secondary messenger reflecting the functional state of the ETC. We also demonstrated that Ald plays a crucial role in maintaining the redox balance of $NADH/NAD^+$ in mycobacteria exposed to severe respiration-inhibitory conditions. On the basis of this finding, we expect the development of a new regimen that improves the efficacy of antitubercular drugs targeting the mycobacterial respiratory ETC.

MATERIALS AND METHODS

Bacterial strains, plasmids, and culture conditions. The bacterial strains and plasmids used in this study are listed in Table 1. *M. smegmatis* strains were grown in Middlebrook 7H9 medium (Difco, Sparks, MD) supplemented with 0.2% (wt/vol) glucose as a carbon source and 0.02% (vol/vol) Tween 80 as an anticlumping agent at 37°C. *M. smegmatis* strains were grown either aerobically in a 500-ml flask filled with 100 ml of 7H9-glucose medium on a gyratory shaker (200 rpm) or under hypoxic conditions in a 250-ml flask filled with 150 ml of 7H9-glucose medium and tightly sealed with a rubber stopper (the ratio of headspace volume to culture volume was 1) on a gyratory shaker (200 rpm) for 20 h following inoculation of the medium with aerobically grown preculture to an optical density at 600 nm (OD_{600}) of 0.05, which enabled a gradual depletion of O_2 from the growth medium. The growth of the *M. smegmatis* WT strain was halted under these hypoxic conditions approximately 20 h after the culture was inoculated (see Fig. S2 in the supplemental material). When methylene blue (0.75 μg/ml) was added to the hypoxic culture of the WT strain as an oxygen indicator, the complete decolorization of methylene blue was observed to occur at between 30 and 31 h after the cultivation was initiated. These observations indicate that the 20-h hypoxic cultures used in this study were under microaerophilic conditions. For the treatment of *M. smegmatis* cultures with KCN, *M. smegmatis* strains were grown to an OD_{600} of 0.5 to 0.6. Following the addition of KCN to the cultures, the strains were further grown for 15 min. To determine the MIC of Q203, *M. smegmatis* strains were grown in 7H9 medium containing 0.5% (wt/vol) bovine serum albumin fraction V, 0.2% (wt/vol) glucose, 0.2% (vol/vol) glycerol, 0.085% (wt/vol) NaCl, and 0.05% (vol/vol) Tween 80 (7H9-ADNaCl). *E. coli* strains were grown in Luria-Bertani (LB) medium at 37°C. Kanamycin (50 μg/ml for *E. coli* and 30 μg/ml for *M. smegmatis*) and hygromycin (200 μg/ml for *E. coli* and 50 μg/ml for *M. smegmatis*) were added to the growth medium when required. The construction of

TABLE 1 Bacterial strains and plasmids used in this study

Strain or plasmid	Relevant phenotype or genotype[a]	Reference or source
Strains		
M. smegmatis		
mc²155	High-transformation-efficiency mutant of *M. smegmatis* ATCC 607	53
Δ*aldR* strain	*MSMEG_2660* (*aldR*) deletion mutant derived from *M. smegmatis* mc²155	61
Δ*ald* strain	*MSMEG_2659* (*ald*) deletion mutant derived from *M. smegmatis* mc²155	This study
Δ*bd* strain	*MSMEG_3233* (*cydA*) deletion mutant derived from *M. smegmatis* mc²155	This study
Δaa_3 strain	*MSMEG_4268* (*ctaC*) deletion mutant derived from *M. smegmatis* mc²155	This study
Δ*bd* Δ*ald* strain	*MSMEG_3233* (*cydA*) deletion mutant derived from *M. smegmatis* Δ*ald*	This study
E. coli DH5α	ϕ80d*lacZ*ΔM15 Δ*lacU169 recA1 endA1 hsdR17 supE44 thi1 gyrA96 relA1*	62
Plasmids		
pKOTs	Hyg^r; pKO-based vector containing a temp-sensitive replication origin (pAL500Ts) and pUC ori	61
pNC	Hyg^r; promoterless *lacZ*	63
pMV306	Km^r; integrative vector containing the *int* and *attP* sites of mycobacteriophage L5 for integration into the mycobacterial genome	64, 65
pNBV1	Hyg^r; 5.8-kb vector derived from p16R1	66
pKOTsΔald	pKOTs::0.81-kb BamHI-HindIII fragment containing Δ*MSMEG_2659* (Δ*ald*)	This study
pKOTsΔbd	pKOTs::0.74-kb NotI-HindIII fragment containing Δ*MSMEG_3233* (Δ*bd*)	This study
pKOTsΔaa_3	pKOTs::0.94-kb BamHI-HindIII fragment containing Δ*MSMEG_4268* (Δaa_3)	This study
pALDLACZ	pNC::0.52-kb XbaI-ClaI fragment containing the *ald* promoter region of *M. smegmatis* mc²155	12
pMV306ctaC	pMV306 with 1.37-kb XbaI-HindIII fragment containing *ctaC* of *M. smegmatis* mc²155	This study
pMV306ald	pMV306 with 1.55-kb XbaI-HindIII fragment containing *ald* of *M. smegmatis* mc²155	This study
pNBV1cydA	pNBV1 with 1.92-kb XbaI-HindIII fragment containing *cydA* of *M. smegmatis* mc²155	This study

[a]Antibiotic resistance is indicated by abbreviation (Hyg, hygromycin; Km, kanamycin).

the mutant strains of *M. smegmatis* and the plasmids used in this study is described in the supplemental material.

DNA manipulation and electroporation. Standard protocols or manufacturers' instructions were followed for recombinant DNA manipulations (52). The introduction of plasmids into *M. smegmatis* strains was conducted by electroporation as previously described (53).

Preparation of membrane fractions and measurement of the oxygen consumption rate. For the isolation of the membrane fractions, 200-ml cultures of *M. smegmatis* strains were grown aerobically to an OD_{600} of 0.7 to 0.8 at 37°C. The harvested cells were then resuspended in 50 mM potassium phosphate (PP) buffer (pH 7.0) and disrupted by five passages through a French pressure cell. The cell-free crude extracts were subsequently obtained by centrifugation twice at 20,000 × *g* for 15 min at 4°C. The membrane fractions were isolated by the ultracentrifugation of crude extracts at 100,000 × *g* for 90 min at 4°C. The prepared membrane fractions were then washed once with PP buffer and resuspended in the same buffer. The oxygen consumption rate was measured polarographically with a YSI 5300 Clark-type electrode (Yellow Springs Instrument Co., Inc., Yellow Springs, OH) by using the resuspended membrane fractions containing 0.2 mg of proteins in 5 ml of PP buffer saturated with ambient air. The reaction was started by the addition of 100 μl of 50 mM NADH as an electron donor, and the oxygen consumption rate was recorded for 100 s at 30°C.

Reverse transcription-PCR and quantitative real-time PCR. RNA isolation from *M. smegmatis* strains, as well as the preparation of cDNA, RT-PCR, and qRT-PCR were conducted as previously described (54). To synthesize cDNA, the following primers were used: RT-16sr(−) (5′-ACAACGCTCG GACCCTAC-3′) for the 16S rRNA gene, R_ald_RT (5′-GCACGGTCTCGTAGGCGATC-3′) for the *ald* gene, R_ctaC_RT (5′-CGTGTCGGTCGCCTTCTTGC-3′) for the *ctaC* gene, and R_cydA_RT (5′-TTCCTGCACGA TGCCGGTCG-3′) for the *cydA* gene. For RT-PCR and qRT-PCR, the following primers were employed: RT-16sr(+) (5′-CTGGGACTGAGATACGGC-3′) and RT-16sr(−) for the 16S rRNA gene, F_ald_RT (5′-C GCCGAGATCGTCAACACCG-3′) and R_ald_RT for the *ald* gene, F_ctaC_RT (5′-GGCTCTGCGCTACTGC TGAG-3′) and R_ctaC_RT for the *ctaC* gene, and F_cydA_RT (5′-CGGTGGCAGTTCGGAATCAC-3′) and R_cydA_RT for the *cydA* gene.

Enzyme assay and protein determination. Cells of *M. smegmatis* were harvested, resuspended in β-galactosidase assay buffer (50 mM potassium phosphate buffer [pH 7.0] containing 10 mM KCl, 1 mM $MgSO_4$, and 10 mM β-mercaptoethanol) or Ald assay buffer (50 mM glycine/KOH [pH 10.2]), and disrupted by five passages through a French pressure cell. The cell-free crude extracts were obtained following centrifugation at 20,000 × *g* for 10 min at 4°C.

The protein concentration was determined using a Bio-Rad (Hercules, CA) protein assay kit and bovine serum albumin as a standard protein.

(i) β-Galactosidase assay. β-Galactosidase activity was assayed spectrophotometrically as previously described (55).

(ii) Ald assay. Ald activity was determined by measuring the initial conversion rate of NAD^+ to NADH accompanying the production of pyruvate from alanine, as previously described (5, 56). The reaction mixture contained 2.5 mM NAD^+, 100 mM L-alanine, 50 mM glycine-KOH (pH 10.2), and appropriate amounts of crude extracts in a final volume of 1 ml. The reaction mixture without crude extracts was

preincubated at 37°C before starting the reaction by the addition of crude extracts. The conversion of NAD^+ to NADH was monitored spectrophotometrically for 3 min at 340 nm.

(iii) Activity staining of Ald. Crude extracts (20 μg) were subjected to nondenaturing PAGE (7.5% [wt/vol] acrylamide). After electrophoresis, the staining of the gel by Ald activity was performed in 50 mM glycine-KOH (pH 10.2) containing 0.064 mM phenazine methosulfate, 0.24 mM nitroblue tetrazolium, and 50 mM L-alanine, as previously described (57). The protein bands with Ald activity were stained purple on the gel.

Determination of the intracellular NADH/NAD^+ ratio. The concentrations of NADH and NAD^+ were determined by a nucleotide cycling assay with modifications (58–60). Briefly, *M. smegmatis* cells corresponding to 1 ml of cultures grown to an OD_{600} of 0.7 were harvested by centrifugation at 15,000 $\times$ *g* for 1 min, and then immediately frozen in a dry ice-ethanol bath. The cell pellets of *M. smegmatis* strains were resuspended in 250 μl of either 0.1 M HCl (for NAD^+) or 0.2 M NaOH (for NADH). The samples were heated for 20 min at 80°C and then cooled on ice. The cell-free supernatants were obtained by centrifugation at 5,000 $\times$ *g* for 5 min and then neutralized by adding 250 μl of 0.2 M NaOH (for NAD^+) or 0.1 M HCl (for NADH). The reaction mixture (1 ml) composed of 100 μl of 1 M bicine buffer (pH 8.0), 100 μl of absolute ethanol, 100 μl of 40 mM EDTA (pH 8.0), 100 μl of 4.2 mM thiazolyl blue tetrazolium bromide ([MTT] ε_{243} = 20.7 $mM^{-1} \cdot cm^{-1}$), 100 μl of 16.6 mM phenazine ethosulfate, and 500 μl of the neutralized sample was preincubated for 3 min at 25°C in a 1-ml cuvette in the dark before the assay. The assay was started by the addition of 30 μl of yeast alcohol dehydrogenase (Sigma, St. Louis, MO), which had been diluted in 0.1 M bicine buffer (pH 8.0) to 334 U/ml, to the reaction mixture. The absorbance at 570 nm was measured for 1 min. A standard curve was generated using standard solutions of NADH or NAD^+ in the concentration range between 0 and 3 μM. The concentration of NAD(H) stock solution was spectrophotometrically determined using an ε_{340} of 6.22 $mM^{-1} \cdot cm^{-1}$ for NADH and an ε_{260} of 16.9 $mM^{-1} \cdot cm^{-1}$ for NAD^+.

Nuclear magnetic resonance analysis. *M. smegmatis* cells were grown either aerobically to an OD_{600} of 0.7 to 0.8 or under hypoxic conditions for 20 h. One hundred milliliters of culture was harvested by centrifugation at 5,000 $\times$ *g* for 5 min at 4°C and washed with 50 ml of 50 mM PP buffer (pH 7.0). The cell pellets were resuspended in 2 ml of ice-cold water and disrupted by five passages through a French pressure cell. The cell-free crude extracts were obtained by centrifugation at 20,000 $\times$ *g* for 15 min at 4°C. Prechilled methanol and chloroform were sequentially added to the crude extracts containing 4 mg of proteins under vigorous vortex at a methanol/chloroform/crude extract ratio of 1:1:1 (vol/vol/vol), and then the mixture was left overnight at −20°C for phase separation. After centrifugation at 4,000 $\times$ *g* for 20 min at 4°C, the aqueous phase (upper phase) was collected and subjected to lyophilization.

The lyophilized samples were redissolved using 500 μl of deuterium oxide (D_2O; 99.9% in D) that includes 2 mM 3-(trimethylsilyl)propionic-2,2,3,3-tetradeuteropropionic acid sodium salt (TSP-d_4) as a reference of chemical shift (0.00 ppm) and quantification. Each sample was transferred to a 5-mm NMR tube (Agilent Technologies, Palo Alto, CA) before NMR measurement.

^{1}H-NMR spectra were acquired using a 600 MHz Agilent NMR spectrometer (Agilent Technologies). A Carr-Purcell-Meiboom-Gill (CPMG) pulse sequence was used to reduce the signals of water and macromolecule. The acquisition time was 2.999 s and the relaxation delay time was 3 s. Overall, 128 transients were collected. All spectra were processed and assigned using Chenomx NMR Suite 7.1 professional with the Chenomx 600 MHz library database (Chenomx Inc., Edmonton, Canada).

MIC assay. *M. smegmatis* WT and Δ*bd*, Δ*ald*, and Δ*bd* Δ*ald* mutant strains were grown in 7H9-ADNaCl to an OD_{600} of 1.0 to 1.2, harvested by centrifugation, washed twice with 7H9-ADNaCl, and diluted in 96-well plates with a starting OD_{600} of 0.01. Q203 was added to final concentrations of 10 to 0.04 μM using 2-fold serial dilutions. Wells containing no Q203 were used as the controls. The plates were incubated at 37°C and the optical density was measured at 600 nm after 48 h. All growth assays were performed in triplicates. The MIC values were calculated by Prism, ver. 5.01 (GraphPad Software Inc., San Diego, CA).

Zone inhibition assay. *M. smegmatis* strains were aerobically grown in 7H9-glucose medium to an OD_{600} of 0.5, 5-ml aliquots of cultures were uniformly spread on 7H9-glucose agar plates, and the rest of the culture was drained off. The remaining culture liquid was removed by tapping the plates on a paper towel. The plates were then dried for 3 h at room temperature, and the paper discs impregnated with 20 μl of 5 mM Q203 were placed on the surface of the dried plates. The plates were incubated for 3 days at 37°C.

SUPPLEMENTAL MATERIAL

Supplemental material for this article may be found at https://doi.org/10.1128/JB.00152-18.

SUPPLEMENTAL FILE 1, PDF file, 0.7 MB.

ACKNOWLEDGMENT

This research was supported by the Basic Science Research Program through the National Research Foundation of Korea (NRF) funded by the Ministry of Education, Science and Technology (NRF-2017R1A2B4008404).

REFERENCES

1. Chen JM, Alexander DC, Behr MA, Liu J. 2003. *Mycobacterium bovis* BCG vaccines exhibit defects in alanine and serine catabolism. Infect Immun 71:708–716. https://doi.org/10.1128/IAI.71.2.708-716.2003.
2. Giffin MM, Modesti L, Raab RW, Wayne LG, Sohaskey CD. 2012. *ald* of *Mycobacterium tuberculosis* encodes both the alanine dehydrogenase and the putative glycine dehydrogenase. J Bacteriol 194:1045–1054. https://doi.org/10.1128/JB.05914-11.
3. Feng Z, Caceres NE, Sarath G, Barletta RG. 2002. *Mycobacterium smegmatis* L-alanine dehydrogenase (Ald) is required for proficient utilization of alanine as a sole nitrogen source and sustained anaerobic growth. J Bacteriol 184:5001–5010. https://doi.org/10.1128/JB.184.18.5001-5010.2002.
4. Betts JC, Lukey PT, Robb LC, McAdam RA, Duncan K. 2002. Evaluation of a nutrient starvation model of *Mycobacterium tuberculosis* persistence by gene and protein expression profiling. Mol Microbiol 43:717–731. https://doi.org/10.1046/j.1365-2958.2002.02779.x.
5. Hutter B, Dick T. 1998. Increased alanine dehydrogenase activity during dormancy in *Mycobacterium smegmatis*. FEMS Microbiol Lett 167:7–11. https://doi.org/10.1111/j.1574-6968.1998.tb13200.x.
6. Giffin MM, Shi L, Gennaro ML, Sohaskey CD. 2016. Role of alanine dehydrogenase of *Mycobacterium tuberculosis* during recovery from hypoxic nonreplicating persistence. PLoS One 11:e0155522. https://doi.org/10.1371/journal.pone.0155522.
7. Usha V, Jayaraman R, Toro JC, Hoffner SE, Das KS. 2002. Glycine and alanine dehydrogenase activities are catalyzed by the same protein in *Mycobacterium smegmatis*: upregulation of both activities under microaerophilic adaptation. Can J Microbiol 48:7–13. https://doi.org/10.1139/w01-126.
8. Agren D, Stehr M, Berthold CL, Kapoor S, Oehlmann W, Singh M, Schneider G. 2008. Three-dimensional structures of apo- and holo-L-alanine dehydrogenase from *Mycobacterium tuberculosis* reveal conformational changes upon coenzyme binding. J Mol Biol 377:1161–1173. https://doi.org/10.1016/j.jmb.2008.01.091.
9. Tripathi SM, Ramachandran R. 2008. Crystal structures of the *Mycobacterium tuberculosis* secretory antigen alanine dehydrogenase (Rv2780) in apo and ternary complex forms captures "open" and "closed" enzyme conformations. Proteins 72:1089–1095. https://doi.org/10.1002/prot.22101.
10. Andersen AB, Andersen P, Ljungqvist L. 1992. Structure and function of a 40,000-molecular-weight protein antigen of *Mycobacterium tuberculosis*. Infect Immun 60:2317–2323.
11. Raynaud C, Etienne C, Peyron P, Laneelle MA, Daffe M. 1998. Extracellular enzyme activities potentially involved in the pathogenicity of *Mycobacterium tuberculosis*. Microbiology 144:577–587. https://doi.org/10.1099/00221287-144-2-577.
12. Jeong JA, Baek EY, Kim SW, Choi JS, Oh JI. 2013. Regulation of the *ald* gene encoding alanine dehydrogenase by AldR in *Mycobacterium smegmatis*. J Bacteriol 195:3610–3620. https://doi.org/10.1128/JB.00482-13.
13. Jeong JA, Hyun J, Oh JI. 2015. Regulation mechanism of the *ald* gene encoding alanine dehydrogenase in *Mycobacterium smegmatis* and *Mycobacterium tuberculosis* by the Lrp/AsnC family regulator AldR. J Bacteriol 197:3142–3153. https://doi.org/10.1128/JB.00453-15.
14. Starck J, Kallenius G, Marklund BI, Andersson DI, Akerlund T. 2004. Comparative proteome analysis of *Mycobacterium tuberculosis* grown under aerobic and anaerobic conditions. Microbiology 150:3821–3829. https://doi.org/10.1099/mic.0.27284-0.
15. Rosenkrands I, Slayden RA, Crawford J, Aagaard C, Barry CE, III, Andersen P. 2002. Hypoxic response of *Mycobacterium tuberculosis* studied by metabolic labeling and proteome analysis of cellular and extracellular proteins. J Bacteriol 184:3485–3491. https://doi.org/10.1128/JB.184.13.3485-3491.2002.
16. Voskuil MI, Visconti KC, Schoolnik GK. 2004. *Mycobacterium tuberculosis* gene expression during adaptation to stationary phase and low-oxygen dormancy. Tuberculosis 84:218–227. https://doi.org/10.1016/j.tube.2004.02.003.
17. Chan K, Knaak T, Satkamp L, Humbert O, Falkow S, Ramakrishnan L. 2002. Complex pattern of *Mycobacterium marinum* gene expression during long-term granulomatous infection. Proc Natl Acad Sci U S A 99:3920–3925. https://doi.org/10.1073/pnas.002024599.
18. Hards K, Robson JR, Berney M, Shaw L, Bald D, Koul A, Andries K, Cook GM. 2015. Bactericidal mode of action of bedaquiline. J Antimicrob Chemother 70:2028–2037. https://doi.org/10.1093/jac/dkv054.
19. Boshoff HI, Barry CE, III. 2005. Tuberculosis - metabolism and respiration in the absence of growth. Nat Rev Microbiol 3:70–80. https://doi.org/10.1038/nrmicro1065.
20. Boshoff HI, Myers TG, Copp BR, McNeil MR, Wilson MA, Barry CE, III. 2004. The transcriptional responses of *Mycobacterium tuberculosis* to inhibitors of metabolism: novel insights into drug mechanisms of action. J Biol Chem 279:40174–40184. https://doi.org/10.1074/jbc.M406796200.
21. Eoh H, Rhee KY. 2013. Multifunctional essentiality of succinate metabolism in adaptation to hypoxia in *Mycobacterium tuberculosis*. Proc Natl Acad Sci U S A 110:6554–6559. https://doi.org/10.1073/pnas.1219375110.
22. Megehee JA, Hosler JP, Lundrigan MD. 2006. Evidence for a cytochrome *bcc-aa*$_3$ interaction in the respiratory chain of *Mycobacterium smegmatis*. Microbiology 152:823–829. https://doi.org/10.1099/mic.0.28723-0.
23. Kana BD, Weinstein EA, Avarbock D, Dawes SS, Rubin H, Mizrahi V. 2001. Characterization of the *cydAB*-encoded cytochrome *bd* oxidase from *Mycobacterium smegmatis*. J Bacteriol 183:7076–7086. https://doi.org/10.1128/JB.183.24.7076-7086.2001.
24. Matsoso LG, Kana BD, Crellin PK, Lea-Smith DJ, Pelosi A, Powell D, Dawes SS, Rubin H, Coppel RL, Mizrahi V. 2005. Function of the cytochrome *bc*$_1$-*aa*$_3$ branch of the respiratory network in mycobacteria and network adaptation occurring in response to its disruption. J Bacteriol 187:6300–6308. https://doi.org/10.1128/JB.187.18.6300-6308.2005.
25. Weinstein EA, Yano T, Li LS, Avarbock D, Avarbock A, Helm D, McColm AA, Duncan K, Lonsdale JT, Rubin H. 2005. Inhibitors of type II NADH: menaquinone oxidoreductase represent a class of antitubercular drugs. Proc Natl Acad Sci U S A 102:4548–4553. https://doi.org/10.1073/pnas.0500469102.
26. Griffin JE, Gawronski JD, Dejesus MA, Ioerger TR, Akerley BJ, Sassetti CM. 2011. High-resolution phenotypic profiling defines genes essential for mycobacterial growth and cholesterol catabolism. PLoS Pathog 7:e1002251. https://doi.org/10.1371/journal.ppat.1002251.
27. McAdam RA, Quan S, Smith DA, Bardarov S, Betts JC, Cook FC, Hooker EU, Lewis AP, Woollard P, Everett MJ, Lukey PT, Bancroft GJ, Jacobs WR, Jr, Duncan K. 2002. Characterization of a *Mycobacterium tuberculosis* H37Rv transposon library reveals insertions in 351 ORFs and mutants with altered virulence. Microbiology 148:2975–2986. https://doi.org/10.1099/00221287-148-10-2975.
28. Miesel L, Weisbrod TR, Marcinkeviciene JA, Bittman R, Jacobs WR, Jr. 1998. NADH dehydrogenase defects confer isoniazid resistance and conditional lethality in *Mycobacterium smegmatis*. J Bacteriol 180:2459–2467.
29. Vilchèze C, Weisbrod TR, Chen B, Kremer L, Hazbon MH, Wang F, Alland D, Sacchettini JC, Jacobs WR, Jr. 2005. Altered NADH/NAD$^+$ ratio mediates coresistance to isoniazid and ethionamide in mycobacteria. Antimicrob Agents Chemother 49:708–720. https://doi.org/10.1128/AAC.49.2.708-720.2005.
30. Awasthy D, Ambady A, Narayana A, Morayya S, Sharma U. 2014. Roles of the two type II NADH dehydrogenases in the survival of *Mycobacterium tuberculosis in vitro*. Gene 550:110–116. https://doi.org/10.1016/j.gene.2014.08.024.
31. Cook GM, Hards K, Vilcheze C, Hartman T, Berney M. 2014. Energetics of respiration and oxidative phosphorylation in mycobacteria. Microbiol Spectr 2:MGM2-0015-2013. https://doi.org/10.1128/microbiolspec.MGM2-0015-2013.
32. Aung HL, Berney M, Cook GM. 2014. Hypoxia-activated cytochrome *bd* expression in *Mycobacterium smegmatis* is cyclic AMP receptor protein dependent. J Bacteriol 196:3091–3097. https://doi.org/10.1128/JB.01771-14.
33. Lee HN, Lee NO, Han SJ, Ko IJ, Oh JI. 2014. Regulation of the *ahpC* gene encoding alkyl hydroperoxide reductase in *Mycobacterium smegmatis*. PLoS One 9:e111680. https://doi.org/10.1371/journal.pone.0111680.
34. Cox RA, Cook GM. 2007. Growth regulation in the mycobacterial cell. Curr Mol Med 7:231–245. https://doi.org/10.2174/156652407780598584.
35. Pethe K, Bifani P, Jang J, Kang S, Park S, Ahn S, Jiricek J, Jung J, Jeon HK, Cechetto J, Christophe T, Lee H, Kempf M, Jackson M, Lenaerts AJ, Pham H, Jones V, Seo MJ, Kim YM, Seo M, Seo JJ, Park D, Ko Y, Choi I, Kim R, Kim SY, Lim S, Yim SA, Nam J, Kang H, Kwon H, Oh CT, Cho Y, Jang Y, Kim J, Chua A, Tan BH, Nanjundappa MB, Rao SP, Barnes WS, Wintjens R, Walker JR, Alonso S, Lee S, Kim J, Oh S, Oh T, Nehrbass U, Han SJ, No Z, Lee J, Brodin P, Cho SN, Nam K, Kim J. 2013. Discovery of Q203, a potent clinical candidate for the treatment of tuberculosis. Nat Med 19:1157–1160. https://doi.org/10.1038/nm.3262.
36. Rao SP, Alonso S, Rand L, Dick T, Pethe K. 2008. The protonmotive force is required for maintaining ATP homeostasis and viability of hypoxic,

nonreplicating *Mycobacterium tuberculosis*. Proc Natl Acad Sci U S A 105:11945–11950. https://doi.org/10.1073/pnas.0711697105.
37. Bhat SA, Iqbal IK, Kumar A. 2016. Imaging the NADH:NAD^+ homeostasis for understanding the metabolic response of *Mycobacterium* to physiologically relevant stresses. Front Cell Infect Microbiol 6:145. https://doi.org/10.3389/fcimb.2016.00145.
38. Watanabe S, Zimmermann M, Goodwin MB, Sauer U, Barry CE, III, Boshoff HI. 2011. Fumarate reductase activity maintains an energized membrane in anaerobic *Mycobacterium tuberculosis*. PLoS Pathog 7:e1002287. https://doi.org/10.1371/journal.ppat.1002287.
39. Koul A, Vranckx L, Dhar N, Gohlmann HW, Ozdemir E, Neefs JM, Schulz M, Lu P, Mortz E, McKinney JD, Andries K, Bald D. 2014. Delayed bactericidal response of *Mycobacterium tuberculosis* to bedaquiline involves remodelling of bacterial metabolism. Nat Commun 5:3369. https://doi.org/10.1038/ncomms4369.
40. Phong WY, Lin W, Rao SP, Dick T, Alonso S, Pethe K. 2013. Characterization of phosphofructokinase activity in *Mycobacterium tuberculosis* reveals that a functional glycolytic carbon flow is necessary to limit the accumulation of toxic metabolic intermediates under hypoxia. PLoS One 8:e56037. https://doi.org/10.1371/journal.pone.0056037.
41. Moraski GC, Markley LD, Hipskind PA, Boshoff H, Cho S, Franzblau SG, Miller MJ. 2011. Advent of imidazo[1,2-α]pyridine-3-carboxamides with potent multi- and extended drug resistant antituberculosis activity. ACS Med Chem Lett 2:466–470. https://doi.org/10.1021/ml200036r.
42. Garnier T, Eiglmeier K, Camus JC, Medina N, Mansoor H, Pryor M, Duthoy S, Grondin S, Lacroix C, Monsempe C, Simon S, Harris B, Atkin R, Doggett J, Mayes R, Keating L, Wheeler PR, Parkhill J, Barrell BG, Cole ST, Gordon SV, Hewinson RG. 2003. The complete genome sequence of *Mycobacterium bovis*. Proc Natl Acad Sci U S A 100:7877–7882. https://doi.org/10.1073/pnas.1130426100.
43. Saxena S, Devi PB, Soni V, Yogeeswari P, Sriram D. 2014. Identification of novel inhibitors against *Mycobacterium tuberculosis* L-alanine dehydrogenase (MTB-AlaDH) through structure-based virtual screening. J Mol Graph Model 47:37–43. https://doi.org/10.1016/j.jmgm.2013.08.005.
44. Saxena S, Samala G, Sridevi JP, Devi PB, Yogeeswari P, Sriram D. 2015. Design and development of novel *Mycobacterium tuberculosis* L-alanine dehydrogenase inhibitors. Eur J Med Chem 92:401–414. https://doi.org/10.1016/j.ejmech.2014.12.046.
45. Lu P, Heineke MH, Koul A, Andries K, Cook GM, Lill H, van Spanning R, Bald D. 2015. The cytochrome *bd*-type quinol oxidase is important for survival of *Mycobacterium smegmatis* under peroxide and antibiotic-induced stress. Sci Rep 5:10333. https://doi.org/10.1038/srep10333.
46. Berney M, Hartman TE, Jacobs WR, Jr. 2014. A *Mycobacterium tuberculosis* cytochrome *bd* oxidase mutant is hypersensitive to bedaquiline. mBio 5:e01275-14. https://doi.org/10.1128/mBio.01275-14.
47. Arora K, Ochoa-Montano B, Tsang PS, Blundell TL, Dawes SS, Mizrahi V, Bayliss T, Mackenzie CJ, Cleghorn LA, Ray PC, Wyatt PG, Uh E, Lee J, Barry CE, III, Boshoff HI. 2014. Respiratory flexibility in response to inhibition of cytochrome *c* oxidase in *Mycobacterium tuberculosis*. Antimicrob Agents Chemother 58:6962–6965. https://doi.org/10.1128/AAC.03486-14.
48. Phummarin N, Boshoff HI, Tsang PS, Dalton J, Wiles S, Barry CE, III, Copp BR. 2016. SAR and identification of 2-(quinolin-4-yloxy)acetamides as *Mycobacterium tuberculosis* cytochrome bc_1 inhibitors. Med Chem Commun 7:2122–2127. https://doi.org/10.1039/C6MD00236F.
49. Kalia NP, Hasenoehrl EJ, Ab Rahman NB, Koh VH, Ang MLT, Sajorda DR, Hards K, Gruber G, Alonso S, Cook GM, Berney M, Pethe K. 2017. Exploiting the synthetic lethality between terminal respiratory oxidases to kill *Mycobacterium tuberculosis* and clear host infection. Proc Natl Acad Sci U S A 114:7426–7431. https://doi.org/10.1073/pnas.1706139114.
50. Rybniker J, Vocat A, Sala C, Busso P, Pojer F, Benjak A, Cole ST. 2015. Lansoprazole is an antituberculous prodrug targeting cytochrome bc_1. Nat Commun 6:7659. https://doi.org/10.1038/ncomms8659.
51. Sassetti CM, Rubin EJ. 2003. Genetic requirements for mycobacterial survival during infection. Proc Natl Acad Sci U S A 100:12989–12994. https://doi.org/10.1073/pnas.2134250100.
52. Sambrook J, Green MR. 2012. Molecular cloning: a laboratory manual, 4th ed. Cold Spring Harbor Laboratory Press, Cold Spring Harbor, NY.
53. Snapper SB, Melton RE, Mustafa S, Kieser T, Jacobs WR, Jr. 1990. Isolation and characterization of efficient plasmid transformation mutants of *Mycobacterium smegmatis*. Mol Microbiol 4:1911–1919. https://doi.org/10.1111/j.1365-2958.1990.tb02040.x.
54. Kim MJ, Park KJ, Ko IJ, Kim YM, Oh JI. 2010. Different roles of DosS and DosT in the hypoxic adaptation of mycobacteria. J Bacteriol 192:4868–4875. https://doi.org/10.1128/JB.00550-10.
55. Oh JI, Kaplan S. 1999. The cbb_3 terminal oxidase of *Rhodobacter sphaeroides* 2.4.1: structural and functional implications for the regulation of spectral complex formation. Biochemistry 38:2688–2696. https://doi.org/10.1021/bi9825100.
56. Ohshima T, Sakane M, Yamazaki T, Soda K. 1990. Thermostable alanine dehydrogenase from thermophilic *Bacillus sphaericus* DSM 462. Purification, characterization and kinetic mechanism. Eur J Biochem 191:715–720.
57. Hutter B, Singh M. 1998. Host vector system for high-level expression and purification of recombinant, enzymatically active alanine dehydrogenase of *Mycobacterium tuberculosis*. Gene 212:21–29. https://doi.org/10.1016/S0378-1119(98)00134-6.
58. Chawla M, Parikh P, Saxena A, Munshi M, Mehta M, Mai D, Srivastava AK, Narasimhulu KV, Redding KE, Vashi N, Kumar D, Steyn AJ, Singh A. 2012. *Mycobacterium tuberculosis* WhiB4 regulates oxidative stress response to modulate survival and dissemination *in vivo*. Mol Microbiol 85:1148–1165. https://doi.org/10.1111/j.1365-2958.2012.08165.x.
59. Leonardo MR, Dailly Y, Clark DP. 1996. Role of NAD in regulating the *adhE* gene of *Escherichia coli*. J Bacteriol 178:6013–6018. https://doi.org/10.1128/jb.178.20.6013-6018.1996.
60. San KY, Bennett GN, Berrios-Rivera SJ, Vadali RV, Yang YT, Horton E, Rudolph FB, Sariyar B, Blackwood K. 2002. Metabolic engineering through cofactor manipulation and its effects on metabolic flux redistribution in *Escherichia coli*. Metab Eng 4:182–192. https://doi.org/10.1006/mben.2001.0220.
61. Jeong JA, Lee HN, Ko IJ, Oh JI. 2013. Development of new vector systems as genetic tools applicable to mycobacteria. J Life Sci 23:290–298. https://doi.org/10.5352/JLS.2013.23.2.290.
62. Jessee J. 1986. New subcloning efficiency competent cell: $>1\times10^6$ transformants/μg. Focus 8:9.
63. Song T, Park SW, Park SJ, Kim JH, Yu JY, Oh JI, Kim YM. 2010. Cloning and expression analysis of the duplicated genes for carbon monoxide dehydrogenase of *Mycobacterium* sp. strain JC1 DSM. 3803. Microbiology 156:999–1008. https://doi.org/10.1099/mic.0.034769-0.
64. Brown AK, Bhatt A, Singh A, Saparia E, Evans AF, Besra GS. 2007. Identification of the dehydratase component of the mycobacterial mycolic acid-synthesizing fatty acid synthase-II complex. Microbiology 153:4166–4173. https://doi.org/10.1099/mic.0.2007/012419-0.
65. Stover CK, de la Cruz VF, Fuerst TR, Burlein JE, Benson LA, Bennett LT, Bansal GP, Young JF, Lee MH, Hatfull GF, Snapper SB, Barletta RG, Jacobs WR, Jr, Bloom BR. 1991. New use of BCG for recombinant vaccines. Nature 351:456–460. https://doi.org/10.1038/351456a0.
66. Howard NS, Gomez JE, Ko C, Bishai WR. 1995. Color selection with a hygromycin-resistance-based *Escherichia coli*-mycobacterial shuttle vector. Gene 166:181–182. https://doi.org/10.1016/0378-1119(95)00597-X.